AD_____

Award Number: W81XWH-07-1-0159

TITLE: Identification and Therapeutic Targeting of Paracrine Senescence Factors in the Prostate Tumor Microenvironment

PRINCIPAL INVESTIGATOR: Dr. James Dean

CONTRACTING ORGANIZATION: Fred Hutchinson Cancer Research Center
Seattle, WA 96109

REPORT DATE: March 2011

TYPE OF REPORT: Annual

PREPARED FOR: U.S. Army Medical Research and Materiel Command
Fort Detrick, Maryland 21702-5012

REPORT DOCUMENTATION PAGE

Form Approved
OMB No. 0704-0188

1. REPORT DATE *(DD-MM-YYYY)*	**2. REPORT TYPE**	**3. DATES COVERED** *(From - To)*

4. TITLE AND SUBTITLE	**5a. CONTRACT NUMBER**
	5b. GRANT NUMBER
	5c. PROGRAM ELEMENT NUMBER
6. AUTHOR(S) E-Mail:	**5d. PROJECT NUMBER**
	5e. TASK NUMBER
	5f. WORK UNIT NUMBER
7. PERFORMING ORGANIZATION NAME(S) AND ADDRESS(ES)	**8. PERFORMING ORGANIZATION REPORT NUMBER**
9. SPONSORING / MONITORING AGENCY NAME(S) AND ADDRESS(ES) U.S. Army Medical Research and Materiel Command Fort Detrick, Maryland 21702-5012	**10. SPONSOR/MONITOR'S ACRONYM(S)**
	11. SPONSOR/MONITOR'S REPORT NUMBER(S)

12. DISTRIBUTION / AVAILABILITY STATEMENT
Approved for Public Release; Distribution Unlimited

13. SUPPLEMENTARY NOTES

14. ABSTRACT

15. SUBJECT TERMS

16. SECURITY CLASSIFICATION OF:			**17. LIMITATION OF ABSTRACT**	**18. NUMBER OF PAGES**	**19a. NAME OF RESPONSIBLE PERSON**
a. REPORT	**b. ABSTRACT**	**c. THIS PAGE**			USAMRMC
U	U	U	UU		**19b. TELEPHONE NUMBER** *(include area code)*

Standard Form 298 (Rev. 8-98)
Prescribed by ANSI Std. Z39.18

Table of Contents

Introduction

Deaths due to prostate cancer- the second leading cause of cancer death in men in the United States - could be prevented with more effective treatments. Overcoming tumor cell resistance to the effects of androgen deprivation and chemotherapies would significantly improve the morbidity and mortality of prostate cancer. We ***hypothesize*** that the induction of cellular senescence in the tumor microenvironment by androgen deprivation and cytotoxic chemotherapy promotes the resistance and survival of carcinoma cells. We further ***hypothesize*** that targeting senescence-associated pro-survival paracrine factors will enhance the effects of these therapies and enhance response rates.

To address these hypotheses, we have three aims: First, to identify senescence changes in prostate tissue induced by androgen deprivation and chemotherapy, specifically focusing on identifying factors with the potential to influence the survival/resistance of neoplastic epithelium via paracrine mechanisms. Second, to evaluate the effects of inhibiting specific senescence-associated pro-survival factors using *in vivo* models. Third, to develop and execute clinical trials designed to inhibit senescence-associated paracrine survival mechanisms and determine if enhanced tumor responses can be achieved.

Body

The following summarizes the research accomplishments of the third year of this proposal, as associated with each task in the Statement of Work.

Technical Objective 1: To determine the effects of chemotherapy and androgen ablation therapy on the frequency, type, and location of senescent cells in the prostate, and to identify changes in levels of senescence-associated signaling molecules found in those tissues.

Objective 1a. *Identify senescent cells in pre- and post-chemotherapy prostate tissues from 58 patients.*

Task 1. Perform histochemical staining of a defined set of senescence biomarkers. (Months 1-6) Partially completed as described in prior annual reports. A tissue microarray has been constructed from the prostatectomy tissues of this clinical trial and will be stained, scored and compared with untreated control tissues to identify and quantitate changes in senescent cell populations.

Task 2. Analyze stained tissues, quantitating frequency of positive staining cells in the epithelium versus stroma, in or near benign versus neoplastic prostate glands. (Months 2-8) Partially completed as described in prior annual reports. Analysis of the above staining will be performed.

Task 3. Perform statistical analyses to determine the significance of staining differences between the various compartments and differences before and after chemotherapy. (Months 2-8) Partially completed as described in prior annual reports. Analyses of the above staining will be performed. Staining of pre-treatment vs. post-treatment tissues can only be performed on frozen tissues and may be undertaken as needed to confirm the staining in the post-treatment formalin-fixed, paraffin-embedded tissues.

Objective 1b. *Identify senescent cells in pre- and post-androgen ablation prostate tissues from 48 patients.*

Task 4. Perform histochemical staining of a defined set of senescence biomarkers. (Months 12-20) – Ongoing. The enrollment and treatment have been completed for this protocol of neoadjuvant androgen ablation therapy given prior to prostatectomy. These tissues will be analyzed in May, with concurrent staining of frozen tissue sections, and collection of laser-captured cells from benign, cancer, stroma in the pre- and post-treatment samples. This concurrent analysis will allow me to combine the standard biomarker of senescence-associated-β-galactosidase (requiring frozen tissue sections) with the quantitative analysis of RNA gene expression levels for genes associated with senescence as defined in our previously published work (Bavik, et al, 2006), and that of others (Untergasser et al, 2002).

Task 5. Analyze stained tissues, quantitating frequency of positive staining cells in the epithelium versus stroma, in or near benign versus neoplastic prostate glands. (Months 13-22)-pending

Task 6. Perform statistical analyses to determine the significance of staining differences between the various compartments and differences before and after chemotherapy. (Months 13-22)-pending

Objective 1c. *Examine senescence-associated signaling molecules in pre- and post-chemotherapy prostate tissues from 58 patients.*

Task 7. Perform histochemical staining of secreted signaling molecules. (Months 3-18) Partially completed as described in prior annual reports. The tissue microarray constructed from the prostatectomy tissues of this clinical trial will be stained, scored and compared with untreated control tissues to identify and quantitate changes in senescent cell signaling molecules.

Task 8. Analyze stained tissues, quantitating staining intensities and locations of positive staining; epithelium versus stroma, in or near benign versus neoplastic prostate glands. (Months 4-20) Partially completed as described in prior reports. Recent work has focused on identification of possible functional effects of altered STC1 levels in the prostate tumor microenvironment. The results are as follows.

Characterization of functional consequences of altered STC1 secretion

Introduction

In prior annual reports, my work characterizing environmental conditions regulating expression of the protein STC1 was described. To recap, STC1 from stromal cells was found to have increased secretion levels in vitro in response to numerous factors, including senescence, increasing serum concentrations, osmotic stress, calcium, phosphate, hypoxia, docetaxel and bleomycin chemotherapies, second messenger inhibitory drugs, and the c-met inhibitor SU11274. STC1 is highly expressed and secreted from primary prostate stromal cells, much less so by PC3 cells, and not at all by LNCaP, BPH1, and primary epithelial cells. Staining of a tissue microarray of aging found a significant increase in neoplastic epithelium compared to benign epithelium. Stromal staining was intermediate and increased with aging, although at a borderline level. Serial section immunohistochemistry demonstrated strong co-localization with neuronal tissues and highly suggested co-localization with fibroblastic stromal markers. Given a model where senescence due to aging or environmental stressors such as chemotherapy treatments induce increased STC1 secretion by the stroma, I sought to evaluate the effects of STC1 on epithelial growth and behaviour.

STC1 effects on Proliferation

The effects of exogenous STC1 on proliferation of LNCaP, Du145 and PC3 cells were tested first. Replicate wells were plated with 5000 cells of each respective cell line either in serum-free media or media containing 10% serum. Subsequently, recombinant purified STC1 (BioVendor Research and Diagnostics Products) or purified goat-anti-STC1 polyclonal antibody (R and D Systems) were added to final concentrations of 0.5 ug/ml or 2 ug/ml, respectively. In addition, ATP signaling has been shown to be affected by STC1 (Block et al, 2010), thus the effects of ATP were tested at final concentrations of 50 or 500 μM, alone and in combination with STC1. Finally, the purified goat-anti-HGF polyclonal antibody (R and D Systems) was used as a control for antibody addition at final concentration of 2 ug/ml. In this fashion the effects of increased STC1 and the effects of decreased/neutralized STC1 were tested. After 3 days of incubation with daily addition of ATP, cell numbers were quantitated with an MTS assay (Promega). As seen in Figure 1, the effects of exogenous STC1 and STC1 neutralization with or without ATP addition were not statistically significant compared to relevant internal controls under serum-free conditions for BPH1, Du145 and PC3 cell lines. Similar results were obtained when cells were treated and grown in 10% serum. Effects were similar across replicate experiments.

STC1 effects on growth under hypoxic conditions

Given the significant induction of STC1 in prostate stromal and PC3 cell lines grown under hypoxic conditions, as well as other stress-inducing environmental conditions, I hypothesized that STC1 might be acting as a survival factor. To test this, recombinant human STC1 or anti-STC1 antibodies as described above were added to replicate wells plated to hold 5000 LNCaP, Du145 or PC3 cells. Duplicate plates were placed into standard atmospheric oxygen-containing incubators or a 1% oxygen-containing hypoxia incubator, respectively. At various time points, plates were removed and cell numbers quantitated using an MTS assay (Promega). Cell proliferation effects under normoxic conditions were as seen in Figure 1 (data not shown). Seen in Figure 2, there were clear effects of hypoxia on cell viability over time in all three cell lines. Contrary to prediction, there was no statistically significant effect consistent with STC1 increase by addition of recombinant protein and decrease by anti-STC1 antibody.

STC1 effects on Chemotherapy Response

To evaluate the effects of STC1 supplementation or neutralization on chemotherapy resistance and/or sensitivity, replicate wells were plated with 5000 cells of the BPH1, LNCaP, Du145, or PC3 cell lines. Six hours later, STC1 and control treatments were started as per proliferation experiments above. Twenty-four hours after plating, cells began treatment with varying concentrations of docetaxel (0-100 nM) or mitoxantrone (0-800 nM) based on IC50 values previously determined for the PC3 cell line of 10 and 100 nM, respectively. Cell numbers were quantitated using the MTS assay (Promega) after 3 days of treatment. No significant effects of STC1 supplementation or neutralization could be discerned in any of the four cell lines relative to internal controls (Du145 not shown) upon docetaxel treatment (Figure 3). Mitoxantrone responses were similarly not significant (data not shown).

STC1 effects on cell motility/wound healing

A wound-healing or "scratch" assay was used to examine the contribution of STC1 to cell motility. Briefly, equal numbers of cells were plated and 24 hours later, a sterile pipet tip was used to denude a zone on the cell culture plate of cells. BPH1, Du145 (data not shown) and PC3 cells were each tested. Wells were treated to supplement or neutralize endogenous STC1 as detailed above. Reference marks were made and photographs of the identical locations were taken at multiple time points after denudation. The distance between the two masses of cells were measured on the resulting photographs and graphed over time. STC1 supplementation and neutralization had no significant or reproducible effect on epithelial cell migration compared to appropriate control conditions (Figure 4). Additional variables tested but not displayed for graph clarity included serum-free conditions, ATP treatment alone or combined with STC1.

STC1 effects on intracrine androgen metabolism

In the ovarian system, STC1 treatment of ovarian granulosa cells suppresses production of progesterone and its metabolic enzymes (Luo et al, 2004). In the prostate, our group (Montgomery et al, 2008) and others (Titus et al, 2005) have demonstrated the persistence of intratumoral androgens and have implicated tumoral steroid hormone metabolic enzyme changes in this process. Given the importance of testosterone in prostate cancer etiology and treatment, I sought to characterize whether STC1 might modulate intratumoral production of androgens. To evaluate this, RNA was purified from the LNCaP, PC3 and Du145 cell lines. Validated quantitative real-time PCR primers were obtained from Dr. Elahe Mostaghel in the Nelson laboratory and used to quantitate changes in the various enzymes known to participate in the interconversion of androgens and their steroid precursors (Figure 5). As predicted, the PC3 and Du145 (data not shown) cell lines generally express much higher levels of these enzymes, as predicted by the castration resistant state of these lines, compared to the androgen-dependence of LNCaP. Unfortunately, STC1 supplementation and neutralization had resulted maximal changes in these enzymes of 25% or less (data not shown), suggesting minimal, if any role for STC1 in these changes.

Task 9. Perform statistical analyses to determine the significance of staining differences between the various compartments and differences before and after chemotherapy. (Months 4-20) Partially completed as described in prior annual reports.

Objective 1d. *Examine senescence-associated signaling molecules in pre- and post-androgen ablation prostate tissues from 48 patients.*

Task 10. Perform histochemical staining of secreted signaling molecules. (Months 12-36)-pending, See above plan described in Objective 1b. Of note, the gene expression changes in secreted molecules which occur with senescence as described in prior annual reports and published in part by our laboratory (Coppe et al, PLOS Biology), will be applied to this set of patients as well to maximize detection of senescence in this population as described in Objective 1b.

Task 11. Analyze stained tissues, quantitating staining intensities and locations of positive staining; epithelium versus stroma, in or near benign versus neoplastic prostate glands. (Months 13-36)-pending

Task 12. Perform statistical analyses to determine the significance of staining differences between the various compartments and differences before and after chemotherapy. (Months 13-36)-pending

Objective 1e. *Correlate observed senescence staining results from Objectives 1a-1d with clinical outcomes and gene expression data.*

Task 13. Collate senescence staining results and clinical outcomes. (Months 4-40) – Partially completed as described in prior annual reports.

Task 14. Collaborate with Nelson laboratory members performing the parallel expression studies to correlate staining patterns with gene expression changes. (Months 4-40) – Partially completed as described in prior annual reports.

Technical Objective 2. To examine resistance of senescence-induced carcinogenesis and tumor progression to the effects of docetaxel and/or the anti-IGF-IR antibody IMC-A12 in a nude mouse xenoplant model.

Objective 2a. *Obtain regulatory approval for animal xenoplant trials.*

Task 15. Write animal protocol for therapy trials. (Months 1-2). This has been completed as described in prior annual reports.

Task 16. Obtain necessary animal review board approval. (Months 2-5). This has been completed as described in prior annual reports.

Objective 2b. *Determine the resistance of senescent-dependent carcinogenesis and early tumors to docetaxel chemotherapy.*

Task 17. Culture cells and prepare cellular recombinants with BPH1 or PC3 and primary prostate stromal cells, senescent, or not. Perform sub-kidney capsule implantation surgeries. After 2 weeks of recovery, treat mice with weekly docetaxel for 3 weeks. 2 months after completion of therapy, sacrifice mice and retrieve xenoplanted kidneys. (Months 5-12) - pending The experimental work proposed in this Objective, as with Objectives 2c and 2d continued to be largely deferred to allow commitment of time and energies into completion of the clinical trial described below in Objective 3a, Task 26, as well as the experimental studies described above.

Task 18. Measure resulting graft sizes, fix and embed the tissues, then stain with Hematoxylin and Eosin and immunohistochemistry. Evaluate for invasiveness, senescent cell populations and neoplastic morphologies. (Months 8-14 - pending)

Task 19. Perform statistical analyses to determine significance of chemotherapy-induced changes in the senescent-stimulated, compared to the pre-senescent recombinants. (Months 10-16) - pending

Objective 2c. *Determine the effect of IMC-A12 on senescent-dependent carcinogenesis and early tumors.*

Task 20. Culture cells and prepare cellular recombinants with BPH1 or PC3 and primary prostate stromal cells, senescent, or not. Perform sub-kidney capsule implantation surgeries. After 2 weeks of recovery, treat mice with thrice weekly IMC-A12 injections continuously for 2 months, then sacrifice mice and dissect out kidneys. (Months 7-12) - pending. For further details please see explanation under Objective 2b, Task 17.

Task 21. Measure resulting graft sizes, fix and embed the tissues, then stain with Hematoxylin and Eosin and immunohistochemistry. Evaluate for invasiveness, senescent cell populations and neoplastic morphologies. (Months 10-14) - pending

Task 22. Perform statistical analyses to determine significance of chemotherapy-induced changes in the senescent-stimulated, compared to the pre-senescent recombinants. (Months 12-18) - pending

Objective 2d. *Determine the senescence-dependent resistance of advanced tumors to docetaxel chemotherapy and its modulation by IMC-A12.*

Task 23. Culture cells and prepare cellular recombinants with BPH1 or PC3 and primary prostate stromal cells, senescent, or not. Perform sub-kidney capsule implantation surgeries. Two months after implantation, treat mice with weekly docetaxel for 3 weeks, with or without IMC-A12 thrice weekly treatments. 3 weeks after completion of therapy, sacrifice mice and dissect out kidneys. (Months 10-18) - pending. For further details please see explanation under Objective 2b, Task 17.

Task 24. Measure resulting graft sizes, fix and embed the tissues, then stain with Hematoxylin and Eosin and immunohistochemistry. Evaluate for invasiveness, senescent cell populations and neoplastic morphologies. (Months 13-20 - pending)

Task 25. Perform statistical analyses to determine significance of chemotherapy-induced changes in the senescent-stimulated, compared to the pre-senescent recombinants. (Months 15-22) - pending

Technical Objective 3: To develop and execute clinical trials evaluating the effectiveness of inhibiting senescence-associated modulators of cancer cell survival in the treatment of prostate cancer. The lead candidate for such targeting is currently IGF1R in the insulin-like growth factor pathway. Other targets identified in Specific Aims/Technical Objectives 1 and 2 may also present opportunities for treatment of more novel targets. Optimal target selection and clinical trial design will be determined during year 2 of the proposal.

Objective 3a*: Participate in the execution and analysis of a Phase II clinical trial inhibiting senescence-associated modulators of cancer cell survival in combination with androgen ablation in the neoadjuvant setting prior to radical prostatectomy. The lead class of modulators are anti-IGF1R antibodies under development by Imclone (IMC-A12) or Pfizer (CP-751,871) which inhibit the insulin-like growth factor pathway. Other candidates/pathways will be considered and optimized during the clinical trial design phase of the project in year 2.*

Task 26. Design Clinical Trial (Months 15-18) Completed. Initial design work was described in prior annual reports. In the last interim, USAMRMC ORP HRPO approval memorandum for the laboratory analyses was received on July 28, 2010, HRPO Log Number A-14104.4.

Task 27. Develop recruitment materials, hold in-service for clinical providers and study coordinator. (Months 18-24) – Completed as described in prior annual reports.

Task 28. Recruit, enroll, and treat patients on study. Monitor and report adverse events. (Months 20-55) – Partially completed. To date, 28 subjects have been enrolled out of a goal enrollment of 29 subjects and 23 subjects have completed prostatectomy. There has been one complete response. There have been no serious or unexpected adverse events related to study treatment.

Task 29. Analyze pre- and post-treatment tissues for changes senescent cell content and senescence-associated signaling molecule expression as described above (Objectives 1a. and 1c.). (Months 24-46) – Since receipt of HRPO approval, analyses of the study sample tissues have been initiated. First, to date, benign, cancer and stromal cell populations have been laser-captured from both biopsy and prostatectomy tissue samples of 10 patients. These continue to be captured on an ongoing basis with the plan to collect complete sets of samples from all study patients. Gene expression will be quantitated and compared between the populations. This will allow the treatment-specific gene expression changes to be identified, then compared and contrasted between the various tissue compartments. In addition, pre- and post-treatment frozen sections from each patient are being acquired/collated/collected for pooled staining analysis. Secondly, a study of the serum samples was commenced to analyze changes in circulating biomarkers predicted to reflect the effects of A12 treatment in the first 18 consecutive accrued patients. Please see the section below for a complete discussion of the methods and results of this analysis.

Task 30. Collate and analyze data. (Months 24-50) – Partially completed. Please see below section for the methods and results obtained in the serum biomarker study of the first 18 consecutive accrued patients.

IGF-1R inhibition combined with Androgen Deprivation: Serum biomarker evidence for on-target efficacy and novel correlation with PSA response.

Methods:

The clinical trial (A12) was designed to accrue 28 patients with localized prostate cancer who were at high risk for relapse after prostatectomy. The primary endpoint for the trial was pathological complete response (pCR) rate with this cohort size designed to provide 80% power to detect an increased pCR rate of 20%, compared to historical controls of 5% in trials of hormone therapy only. Treatment consisted of three months of treatment with goserelin (10.8 mg SQ once), bicalutamide (50 mg PO daily) and IMC-A12 (10mg/kg IV every 2 weeks). Tissue and serum acquisition was an integral component of trial design with pre-treatment serum collection as well as mandatory prostate biopsy for the sole purpose of research analyses. Serum samples were collected throughout treatment and at the time of prostatectomy. Prostate tissues excess to the needs of clinical diagnosis were collected at the time of prostatectomy.

For the purposes of a control population, serum samples similarly collected from one treatment cohort of a concurrent clinical trial of neoadjuvant hormone therapy only (NeoADT) (detailed in Objectives 1b and 1d) were similarly analyzed. Pre-treatment values provided an internal control comparison. Blood glucose, serum PSA and testosterone levels were measured in a CLIA-certified clinical pathology laboratory using certified methods. Commercial ELISA assays were used per manufacturer's instructions to assay the serum levels of human growth hormone (R and D systems), insulin (Invitrogen), c-peptide of insulin (Diagnostic Systems Labs). Custom in-house ELISA assays were used to quantitate levels of IGF-I, IGF-II, IGFBP-3, and IGFBP-1 using the respective purified recombinant protein standards, monoclonal antibodies and biotinylated polyclonal antibodies from R and D systems. Samples were measured in duplicate and colorimetric methods used to quantitate protein levels versus a standard curve of purified standard protein. Inter- and intra-assay coefficients of variation ranged from 3-10% for these assays.

The clinical laboratory results and patient demographics were anonymized and linked with the ELISA results by study personnel then the linked data were subjected to further statistical and other analyses with as described below.

Results:

Cohort Demographics and Clinical Outcomes

As designed, the study is accruing a population of prostate cancer patients at high risk of relapse after prostatectomy with median PSA of 12, diagnostic biopsy Gleason score of 4+4, and clinical stage of T2a (Table 1). The control population was designed to be a more intermediate-risk population and this is reflected in the lower PSA (5.2) and Gleason score (4+3) especially. For later analyses, pre-treatment body mass index (BMI) becomes relevant and the two populations were of similar obesity and both on the borderline between "overweight" and "obese" as defined by the BMI.

Clinical pathological outcomes in this initial 18 patient cohort were limited to one complete response (Table 2). Tumor stage outcomes in the remaining patients corresponded to Kattan nomogram predictions (nomograms.org). In a similar fashion, the frequency of lymph node positivity was similar to Kattan nomogram predictions (6/18). Unfortunately, a substantial fraction of the patients (4/18) had positive surgical margins.

Grade 1 or 2 adverse events which were possibly or probably related to A12 therapy included 2 patients who required metformin therapy to treat significant treatment-induced hyperglycemia/diabetes (Table 2). Other adverse events included skin rash, pruritis, dry skin, diarrhea, elevated aspartate transaminase, hypertension, increased lacrimation, blurry vision, scotomata, flashing lights, tinnitus, anemia, thrombocytopenia, and neutropenia. There were no probably or even possibly related Grade 3 or 4 adverse events. Unrelated adverse events included perioperative stroke, post-operative deep venous thrombosis with asymptomatic pulmonary embolism and hypertension.

Effects of A12 plus hormonal therapy on IGF pathway homeostasis biomarkers: On-target efficacy

The IGF-1R is found in tissues throughout the body, including the pituitary. Normal homeostasis of the IGF pathway relies on feedback inhibition by IGF-I signaling through the pituitary IGF-1R (Gualberto et al, 2009). Loss of this feedback inhibition would be predicted to have effects on this homeostasis at multiple levels. As seen in Figure 6, upon A12 treatment, loss of this feedback inhibition leads to dramatically increased circulating levels of growth hormone compared to pre-treatment levels (8.1-fold, $p<0.002$) as well as the NeoADT cohort (3.3-fold, $p<0.004$). The predicted consequences of increased growth hormone include increases in IGF-I, IGF-II, IGFBP-3 and blood glucose levels. In fact, statistically significant increases are seen compared to pre-treatment levels and the hormone therapy-only cohort in IGF-I (3.1-fold $p<0.0001$, 4.5-fold $p<0.0001$), IGF-II (1.5-fold $p<0.006$, 1.9-fold $p<0.0001$) and IGFBP-3 (1.8-fold $p<0.003$, 1.9-fold $p<0.0001$). Together, these data strongly imply that IGF-1R signaling is being effectively inhibited by A12 with hormonal therapy in this patient population.

Effects of A12 plus hormonal therapy on glucose homeostasis biomarkers: Insulin resistance

Blood glucose is an additional factor predicted to be increased by elevated growth hormone levels. However, blood glucose increases are normally tightly controlled by secondary homeostatic mechanisms, including compensatory insulin increases. Clinically, elevations of

blood glucose have been frequently observed in clinical trials across the various anti-IGF-1R therapeutics in development, including A12 (Gualberto et al, 2009). As seen in Figure 7, there are small and non-significant increases in blood glucose of approximately 15 points in the A12-treated patients, compared to pre-treatment values (1.15-fold p=0.18). Blood glucose is also increased compared to the NeoADT cohort (1.22-fold p=0.11). Notably, these were not fasting glucose levels and samples were not drawn at consistent times of the day relative to food ingestion patterns. Thus, these results should be considered with caution as a rough estimate of glucose alterations.

By contrast, insulin and its corresponding c-peptide of insulin were both much more substantially elevated (Figure 7). The elevations of insulin upon A12 treatment were non-significant due to high degrees of measurement variability, but were increased 3.8-fold compared to pre-treatment values (p=0.19) and 5-fold compared to the NeoADT cohort (p=0.06). C-peptide of insulin elevations were somewhat less dramatic, but more statistically significant (2.1-fold, $p<0.005$ versus pre-treatment values; 1.9-fold, $p<0.04$ versus NeoADT values), likely because the longer half-life of c-peptide in the blood reduces variability induced by random differences in food intake. These elevations of insulin and c-peptide in combination with the small increases in blood glucose are consistent with increased peripheral insulin resistance induced by treatment with IMC-A12.

Lastly, IGFBP-1 protein levels would be predicted to decrease in response to increasing levels of insulin secretion seen with A12 treatment (Gualberto, et al, 2009). This is due to negative feedback regulation of IGFBP-1 production in the liver by insulin. However, no decrease is seen upon A12 treatment in our samples. In fact, there is a non-significant increase in IGFBP-1 levels compared to pre-treatment values (2-fold, p=0.14) (Figure 7). Secondly, the baseline levels of IGFBP-1 were lower on average in patients on the A12 study compared to the NeoADT cohort, a relative difference which persisted and increased to a significant 0.37-fold ($p<0.02$) level by the end of study. It should also be noted that the inverse was true when baseline IGF-II levels were compared between the two studies (Figure 6), although in the case of IGF-II, little increase was seen in the NeoADT cohort during treatment, while there were significant increases with A12 treatment as discussed above. The IGFBP-1 changes are most consistent with A12-induced insulin insensitivity in the liver.

In sum, changes in serum insulin, c-peptide and glucose are all consistent with those effects predicted by effective IGF-1R blockade. The IGFBP-1 effects bear further examination, but the simplest explanation is that insulin sensitivity is reduced in the liver, preventing the expected IGFBP-1 decreases with A12 treatment-associated increased insulin levels. In a similar fashion, lack of proportionality between blood glucose changes and the insulin/c-peptide changes suggests the possibility of A12-induced peripheral insulin resistance resulting in substantially increased insulin levels need to achieve similar levels of blood glucose control. This is also consistent with A12-induced diabetes in two of the A12 patients, which was readily controlled with metformin, an insulin-sensitizer.

<u>Correlations of serum biomarkers with clinical PSA outcomes: Discovery of biomarkers of response to IGF-1R inhibition</u>

In general, PSA responses to the combination of A12 and hormonal therapy were excellent, with nadir PSA values at 0.1%-3.5% of initial values. Castrate testosterone levels were achieved in all patients. In absolute terms, nadir PSA values ranged from 0.02 to 2.5 (Median = 0.13) as depicted in Figure 8. In an initial exploratory analysis, A12 patients were stratified into

2 groups based on median nadir PSA- low PSA or better responders and high PSA or worse responders. For most of the biomarkers described above, no quantitative or statistically significant differences were seen, as illustrated by growth hormone levels (Figure 8). This has the interesting implication that PSA responses in these patients are not due to differences in A12 on-target efficacy. Alternatively, there may be subtle differences in anti-IGF-1R activity that these biomarkers are insensitive to, or differences between anti-IGF-1R effectiveness in the pituitary versus the prostate.

By contrast, in the case of insulin and c-peptide of insulin, PSA stratification revealed significant differences in the secreted levels of these factors. Patients with better response to therapy (low PSA group) had very little increase in insulin, while the patients with lesser therapy responses (high PSA group) had substantial insulin increases, nearly 5.3-fold ($p<0.02$) higher (Figure 8). As expected, the c-peptide of insulin was also higher (2.1-fold, $p<0.002$) in the high PSA group, compared to patients with better PSA responses. Interestingly, despite the increased insulin and c-peptide levels, the blood glucoses were also non-significantly higher in the patients with lesser responses to therapy, compared to the low PSA group (1.3-fold, $p=0.14$). By contrast, as observed above, there were no significant differences in the IGFBP-1 levels seen in these two groups despite the significant differences in circulating insulin levels (Figure 8).

Thus, the worse-responding patients appear to account for majority of A12-induced insulin resistance changes seen when cohort is analyzed as one group. Together, these data intriguingly suggest that patients with greater A12-induced insulin insensitivity will have lesser responses to IGF-1R inhibition. If this is the case, then insulin changes in response to IGF-1R inhibitor therapy may allow prediction of response to such therapy. To our knowledge, this is the first reported biomarker of response to this class of agents. Of note, PSA responses did not correlate with IGF-I or IGF-II changes, altered levels of which have previously been correlated with or implicated in therapy resistance mechanisms (Garofalo et al, 2011; Gualberto et al, 2011). Thus, in the case of prostate cancer, the significance of these biomarkers is substantially less than that of the insulin/c-peptide changes.

Body mass index, clinical responses, and biomarker effects

Body mass index and other factors associated with the metabolic syndrome and insulin resistance have been repeatedly linked to prostate cancer development rates, aggressiveness of disease, and even survival (Albanes et al, 2009; Ma, et al, 2008). Above, we have clearly established that A12 treatment results in elevated levels of insulin without corresponding decreases in IGFBP-1, and out of proportion to blood glucose changes. This directly implies A12-induced peripheral and liver insulin resistance. Secondly, our exploratory analyses have shown that patients with better PSA responses to A12 treatment do not have the significant insulin/c-peptide increases seen in patients with lesser PSA responses. To seek further understanding of this issue, the effects of pre-treatment body mass index (BMI) in this trial were evaluated.

The median pre-treatment BMI (29.7) in the A12 population was similar to that in the NeoADT cohort (BMI=28) (Table 1). Given the biomarker changes described above, it would be predicted that the lesser-responding patients (high PSA group) would have a higher BMI. In fact, when compared, pre-treatment BMI values averaged 28.1 for the low PSA group and 32.2 for the high PSA group ($p=0.10$) (Figure 9). Although non-significant, the trend is clear. Unfortunately, pre-treatment BMI could not predict for nadir PSA response ($p=0.70$, data not shown), thus pre-treatment BMI alone is not sufficient to predict response to A12.

Also as expected, the low BMI patients had lesser changes in insulin (0.25x, p=0.06) and c-peptide (0.78, p=0.06) (Figure 9) compared to the high BMI group in response to A12 treatment (although these were of borderline statistical significance). Most interestingly, both groups had a similar lack of IGFBP-1 decreases in response to insulin, but the pre-treatment levels were substantially different. The low BMI group had significantly higher baseline IGFBP-1 levels compared to the high BMI group (4.1x, $p<0.03$), consistent with less pre-treatment insulin resistance in the low BMI group (Figure 9).

A particularly interesting conclusion which can be drawn from this data is that there are inherent differences between pre-treatment, baseline insulin resistance as shown by differences in baseline IGFBP-1 levels which do not correlate with PSA response, and the insulin resistance which is induced on treatment with A12 and which does correlate with PSA response. This suggests possible biological differences between these processes and invites further investigation to characterize these differences.

Conclusions:

Serum biomarkers of the IGF pathway provide strong evidence supporting on-target efficacy of A12 combined with ADT, both compared to pre-treatment controls, and compared to an ADT-only control cohort. Serum biomarkers also suggest peripheral insulin resistance and novel evidence of liver insulin resistance. Exploratory analyses comparing patients with PSA nadir responses above versus below the median find no differences in the biomarkers of on-target efficacy. Despite this, a novel correlation has been discovered suggesting induction of insulin resistance by A12 is linked with with worse responses to the therapy (higher nadir PSA values). Pre-treatment BMI tends to be higher in the patients who respond less well to A12, but pre-treatment BMI can not predict for PSA response. Given a significant correlation of A12-induced insulin resistance with PSA response, the lack of PSA response correlation with pre-treatment IGFBP-1 levels strongly suggests differences between pre-treatment and A12-induced insulin resistance states. Finally, the strong correlation of pre-treatment IGFBP-1 with pre-treatment BMI - and the lack of correlation with PSA response - may provide insight into the limitations of BMI as a pre-treatment A12 predictive biomarker.

Objective 3b: *Design and execute a clinical trial combining docetaxel chemotherapy with an inhibitor of senescence-associated modulation of cancer cell survival in the neoadjuvant setting prior to radical prostatectomy. The anti-IGF1R antibodies such as IMC-A12 (Imclone) or CP-751,871 (Pfizer) are currently the lead candidates for inhibition. Other candidates/pathways will be considered and optimized during the clinical trial design phase of the project in year 3.*

Task 31. Write the protocol and required regulatory documents. (Months 24-30) - pending

Task 32. Obtain regulatory approval from Institutional Review Board. (Months 30-34) - pending

Task 33. Develop recruitment materials, hold in-service for clinical providers and study coordinator. (Months 34-36) - pending

Task 34. Recruit, enroll, and treat patients on study. Monitor and report adverse events. (Months 36-60) - pending

Task 35. Analyze pre- and post-treatment tissues for changes senescent cell content and senescence-associated signaling molecule expression as described above (Objectives 1a. and 1c.). (Months 40-55) - pending

Task 36. Collate and analyze data. (Months 34-60) - pending

Technical Objective 4: To complete data analyses, compile accomplishments and reportable outcomes, and write final project reports and manuscripts.

Objective 4a*: Prepare manuscript 1.*

Task 37. Describe changes in the extent and distribution of senescent cells in the prostate as a function of chemotherapy and androgen ablation therapies. Correlate with alterations in senescence-associated signaling molecules, gene expression studies and clinical outcome measures. (Months 38-44) – Ongoing. A manuscript characterizing the regulation of STC1 secretion levels in response to various environmental conditions as described in prior annual reports has been prepared and is being edited by my mentor, Dr. Peter Nelson. This data was presented in part at the AACR Annual Meeting, 2007, and in updated form at the PCRP IMPACT meeting, March 2011.

Objective 4b: *Prepare manuscript 2.*

Task 38. Describe the effects of docetaxel, mitoxantrone, and IMC-A12 treatment on the nude mouse model of senescence-dependent carcinogenesis and progression. Inter-correlations of presence or absence of tumor, size of grafts, extent and distribution of senescent cells and levels of senescence-associated signaling molecules. (Months 24-30) - pending

Objective 4c*: Prepare manuscript 3.*

Task 39. Describe the clinical efficacy, side effect profile, and laboratory correlates data resulting from the combination of IMC-A12 with androgen ablation. (Months 50-60) – Ongoing. As detailed above, this data comprises the first manuscript which is in the process of preparation at the current time. The included data was presented in large part at the Genitourinary Cancers Symposium, February 2011.

Subsequent planned manuscripts stemming from this trial and laboratory analyses will include characterization of the clinical pathological effects of this treatment, tissue immunohistochemistry to directly evaluate the effects of this treatment on various proteins (including but not limited to senescence-associated-β-galactosidase, androgen receptor, IGF-1R, signaling molecules downstream of IGF-1R, etc.), and gene expression analyses from both an unbiased global perspective as well as analyses focused on androgen responsive genes, a gene signature developed in prostate cancer xenografts treated with A12, and others of interest.

Objective 4d*: Prepare manuscript 4.*

Task 40. Describe the clinical efficacy, side effect profile and laboratory correlate study results from the clinical trail combining IMC-A12 with chemotherapy. (Months 54-60) - pending

Key Research Accomplishments

Potential functional roles for STC1 in the prostate microenvironment were investigated in detail during this interim.

• Modulation of STC1 levels by addition of recombinant purified STC1 and by addition of anti-STC1 polyclonal antibodies were found to not affect proliferation of LNCaP, Du145 or PC3 cells, alone, or with ATP, with or without serum.

• STC1 modulation also did not significantly alter LNCaP, Du145 or PC3 cell proliferation/survival when grown under hypoxic conditions.

• Chemotherapy responses of BPH1, LNCaP, Du145 or PC3 cells to docetaxel or mitoxantrone were not affected by modulation of STC1 levels.

• BPH1, Du145 and PC3 cellular motility in a wound healing assay were not altered by STC1 modulation in the presence or absence of ATP.

• Although I demonstrated substantial and consistent upregulation of steroidogenic enzymes in the castration-resistant cell lines Du145 and PC3 compared to the androgen-dependent cell line LNCaP, there were no significant alterations evident after modulation of STC1 levels.

<u>Initial laboratory analyses of the first 18 consecutive patients accrued to the neoadjuvant clinical trial of IMC-A12 plus ADT were completed with novel findings.</u>

• The desired high risk population is being accrued to the clinical trial, the treatment has been well-tolerated, but the clinical benefits have been minimal. Only 1 patient remains to be accrued and the rest of the prostatectomies will be complete in the next 2 months.

• Laser capture microdissection of the stromal, benign epithelial, and cancerous epithelial compartments has begun from both pre-treatment biopsy tissue, as well as post-treatment prostatectomy tissue.

• Serum biomarkers interrogating alterations in homeostasis of the IGF pathway are consistent with on-target efficacy of this combined treatment. Stratification of the patients based on nadir PSA suggests that the PSA differences are not due to differences in on-target efficacy

• The biomarkers of the glucose-insulin homeostatic pathway are consistent with A12-induced peripheral, as well as liver insulin resistance. Even more interestingly, the bulk of elevations of insulin and c-peptide occur largely in the patients who have higher nadir PSA levels. Thus, higher levels of peripheral insulin resistance induced by A12 are correlated with the clinical PSA outcome in response to A12 treatment. In addition to being one of the first biomarkers of response to IGF-1R inhibitors, this also is suggestive of possible mechanisms of resistance to these inhibitors.

• As predicted, body mass index in the PSA response groups correlated with the insulin resistance of each respective group. Unfortunately, pre-treatment BMI could not predict for PSA outcome.

• Although there was very little difference in IGFBP-1 levels comparing the PSA outcome groups, stratification by BMI identified significant differences in baseline IGFBP-1 levels, consistent with the predicted differences in average circulating insulin levels due to higher peripheral insulin resistance in higher BMI patients.

• The differences between baseline peripheral insulin resistance and A12-induced peripheral and liver insulin resistances, as well as the different patterns of resistance seen when stratifying by PSA compared to BMI would indicate that additional factors likely play a role in overall response to IGF-1R inhibitors.

• Work on Objective 2 has been again been deferred to allow further work on Objectives 1 and 3.

Reportable Outcomes

Abstract:
Dean JP, Coleman I, Sun Y, Martin D, Nelson P. Identification and Characterization of STC1 as a Paracrine Senescence Factor in the Prostate Tumor Microenvironment. Innovative Minds in Prostate Cancer Today (IMPaCT) Conference, Orlando, FL. March 2011.

Dean JP, Montgomery B, Wan J, Cohen P, Haugk K, Corman JM, Ellis WJ, Dalkin BL, Ludwig DL, Plymate SR. On-target activity of neoadjuvant cixutumumab and combined androgen deprivation therapy for high-risk prostate cancer, a phase II trial.
2011 Genitourinary Cancers Symposium, Orlando, FL. February 2011.

Plymate, S, Cohen, P, Dean J, Lin, D, Ludwig, DL, Montgomery, RB. Serum markers of response in a neo-adjuvant clinical trial of the IGF-IR mabA12 in prostate cancer. Fifth International Congress of the GRS and the IGF Society, New York, NY. October 2010.

Dean JP, Plymate SR, Dalkin BL, Ellis WJ, Lin DW, Wright, JW, Corman, JM, Lange PH, True, LD, Montgomery, B. Neoadjuvant IMC-A12 and combined androgen deprivation with prostatectomy for high risk prostate cancer, a phase II trial, Clinical Trials in Progress, ASCO Annual Meeting, June 2010.

Chapter:
Montgomery RB, Dean J, Plymate S. 2010. The role of Insulin-like Growth Factor signaling in prostate cancer development and progression, Smith J (ed) IGFR in Cancer. Springer, NY, NY. 2011 (in press).

Conclusion

The research accomplished during this interim has attempted to characterize the possible functional consequences of increased STC1 in the prostate microenvironment in response to the broad variety of stressful conditions described in prior annual reports. Unfortunately, neither increased STC1 nor decreased STC1 were found to cause significant changes in proliferation,

survival under hypoxic conditions, response or sensitivity to chemotherapy, cell motility/wound healing, or modulation of intracrine androgen metabolism.

Accrual to the clinical trial of neoadjuvant androgen deprivation is finally complete and frozen sections will be stained and gene expression signatures of senescence will be evaluated in the next several months.

Accrual to the neoadjuvant IMC-A12 clinical trial is virtually complete. Initial studies of serum biomarkers have revealed good evidence for on-target efficacy and treatment-induced peripheral and liver insulin resistance. Stratification of patients into response groups based on nadir PSA suggests response may not be due to lack of on-target efficacy, but lined to differences in treatment-induced peripheral insulin resistance. Pre-treatment body mass index was found to be correlated with PSA response but not sufficient to predict for PSA response. By contrast, pre-treatment BMI did correlate very well with baseline differences in insulin resistance- much more so than PSA response.

Together, these studies continue to define novel aspects of the prostate microenvironment and how senescence-associated factors may play an important role in prostate tumor biology and response to therapies.

References

Albanes D, Weinstein SJ, Wright ME, Männistö S, Limburg PJ, Snyder K, Virtamo J. Serum insulin, glucose, indices of insulin resistance, and risk of prostate cancer. J Natl Cancer Inst. 2009 Sep 16;101(18):1272-9.

Bavik C, Coleman I, Dean JP, Knudsen B, Plymate S, Nelson PS. The gene expression program of prostate fibroblast senescence modulates neoplastic epithelial cell proliferation through paracrine mechanisms. Cancer Res. 2006 Jan 15;66(2):794-802.

Block GJ, DiMattia GD, Prockop DJ. Stanniocalcin-1 regulates extracellular ATP-induced calcium waves in human epithelial cancer cells by stimulating ATP release from bystander cells. PLoS One. 2010 Apr 20;5(4):e10237.

Coppé JP, Patil CK, Rodier F, Sun Y, Muñoz DP, Goldstein J, Nelson PS, Desprez PY, Campisi J. Senescence-associated secretory phenotypes reveal cell-nonautonomous functions of oncogenic RAS and the p53 tumor suppressor. PLoS Biol. 2008 Dec 2;6(12):2853-68.

Gualberto A, Pollak M. Emerging role of insulin-like growth factor receptor inhibitors in oncology: early clinical trial results and future directions. Oncogene. 2009 Aug 27;28(34):3009-21.

Gualberto A, Hixon ML, Karp DD, Li D, Green S, Dolled-Filhart M, Paz-Ares LG, Novello S, Blakely J, Langer CJ, Pollak MN. Pre-treatment levels of circulating free IGF-1 identify NSCLC patients who derive clinical benefit from figitumumab. Br J Cancer. 2011 Jan 4;104(1):68-74.

Garofalo C, Manara MC, Nicoletti G, Marino MT, Lollini PL, Astolfi A, Pandini G, López-Guerrero JA, Schaefer KL, Belfiore A, Picci P, Scotlandi K. Efficacy of and resistance to anti-IGF-1R therapies in Ewing's sarcoma is dependent on insulin receptor signaling. Oncogene. 2011 Jan 31. [Epub ahead of print]

Huang F, Hurlburt W, Greer A, Reeves KA, Hillerman S, Chang H, Fargnoli J, Graf Finckenstein F, Gottardis MM, Carboni JM. Differential mechanisms of acquired resistance to insulin-like growth factor-i receptor antibody therapy or to a small-molecule inhibitor, BMS-754807, in a human rhabdomyosarcoma model. Cancer Res. 2010 Sep 15;70(18):7221-31.

Luo CW, Kawamura K, Klein C, Hsueh AJ. Paracrine regulation of ovarian granulosa cell differentiation by stanniocalcin (STC) 1: mediation through specific STC1 receptors. Mol Endocrinol. 2004 Aug;18(8):2085-96.

Ma J, Li H, Giovannucci E, Mucci L, Qiu W, Nguyen PL, Gaziano JM, Pollak M, Stampfer MJ. Prediagnostic body-mass index, plasma C-peptide concentration, and prostate cancer-specific mortality in men with prostate cancer: a long-term survival analysis. Lancet Oncol. 2008 Nov;9(11):1039-47.

Montgomery RB, Mostaghel EA, Vessella R, Hess DL, Kalhorn TF, Higano CS, True LD, Nelson PS. Maintenance of intratumoral androgens in metastatic prostate cancer: a mechanism for castration-resistant tumor growth. Cancer Res. 2008 Jun 1;68(11):4447-54.

Titus MA, Schell MJ, Lih FB, Tomer KB, Mohler JL. Testosterone and dihydrotestosterone tissue levels in recurrent prostate cancer. Clin Cancer Res. 2005 Jul 1;11(13):4653-7.

Ulanet DB, Ludwig DL, Kahn CR, Hanahan D. Insulin receptor functionally enhances multistage tumor progression and conveys intrinsic resistance to IGF-1R targeted therapy. Proc Natl Acad Sci U S A. 2010 Jun 15;107(24):10791-8.

Untergasser G, Koch HB, Menssen A, Hermeking H. Characterization of epithelial senescence by serial analysis of gene expression: identification of genes potentially involved in prostate cancer. Cancer Res. 2002 Nov 1;62(21):6255-62.

Appendices
none

Supporting Data

FIGURE 1. Effects of STC1 modulation on cell proliferation. Equal numbers of the indicated cell line were plated into 96 well plates, treated with the indicated treatment for 3 days, then MTS assay used to quantitate relative cell numbers. Data represent averages of quadruplicate wells and standard deviation.

FIGURE 2. Effects of STC1 modulation on growth in Hypoxia. Equal numbers of the indicated cell line were plated into 96 well plates, treated with the indicated treatment and incubated

under hypoxic (1% Oxygen) conditions with MTS assay used to quantitate relative cell numbers across 6 days. Data represent averages of quadruplicate wells and standard deviation.

FIGURE 3. Effects of STC1 modulation on chemotherapy response. Equal numbers of the indicated cell line were plated into 96 well plates, treated with the indicated STC1-modulating treatment overnight, then docetaxel or mitoxantrone at the indicated concentrations (nM) were added. MTS assay was used to quantitate relative cell numbers after 3 days of treatment. Data represent averages of quadruplicate wells and standard deviation.

FIGURE 4. Effects of STC1 modulation on cell migration. Indicated cell lines were grown to 90%+ confluency then a sterile pipet tip was used to denude a central region. After careful rinsing, growth media containing the indicated treatment was added to the plate. Marked locations were serially photographed at the indicated times and migration of the cell fronts into the denuded area was measured on photographic prints. Data represent averages of quadruplicate wells and standard deviation.

FIGURE 5. Expression of androgen metabolic genes by PC3 and LNCaP cell lines. After isolation and reverse transcription of RNA from the indicated cell lines, relative quantities of the indicated enzymes were quantitated by real-time PCR. Once normalized to RPL13a, levels from the PC3 cell line were compared with the LNCaP expression levels. Red “up” arrows denote enzymes with increased message in PC3 relative to LNCaP and green “down” arrows indicated decreased message in PC3 relative to LNCaP.

TABLE 1. Study patient characteristics. Clinical characteristics of the initial consecutive 18 patients on the neoadjuvant study of IMC-A12 with androgen deprivation are listed. This is the cohort from whom serum biomarkers were assayed and are described in this manuscript. In addition, the clinical characteristics of a control study of neoadjuvant androgen deprivation therapy-only are shown. These characteristics are stratified into clinically relevant groups and the median is described.

TABLE 2. Clinical pathological and Adverse event outcomes. The clinical pathological effects of the neoadjuvant IMC-A12 treatment regimen are listed and compared to predications made by the Kattan pre-operative clinical nomogram. The adverse events noted in patients on the neoadjuvant IMC-A12 clinical trial are listed, categorized by severity (Grade) and ascribed relatedness.

FIGURE 6. Effects of IGF-1R blockade and hormone therapy on IGF pathway homeostasis. ELISA assays were used to quantitate the indicated protein factor from serum obtained prior to treatment (Entry) or at the time of IMC-A12 infusion # 1, 3 or 5 (A12 #1, A12 #3, A12 #5) and at the time of prostatectomy (RRP). Patient samples are from the IMC-A12 study (A12) are shown in blue and neoadjuvant hormonal therapy only (NeoADT). Each data point represents the average value with SEM errors. Fold-change is calculated as A12 average divided by NeoADT average. Statistical 2-sample, 2-tailed t-tests are applied to compare the values indicated by asterisks to determine p-values.

FIGURE 7. Effects of IGF-1R blockade and hormone therapy on glucose homeostasis and insulin activity. ELISA assays were used to quantitate the insulin, c-peptide of insulin and IGFBP-1 levels from serum obtained prior to treatment (Entry) or at the time of IMC-A12 infusion # 1, 3 or 5 (A12 #1, A12 #3, A12 #5) and at the time of prostatectomy (RRP). Blood glucose at these time points was determined by clinical laboratory testing. Patient samples are from the IMC-A12 study (A12) are shown in blue and neoadjuvant hormonal therapy only (NeoADT). Each data point represents the average value with SEM errors. Fold-change is calculated as A12 average divided by NeoADT average. Statistical 2-sample, 2-tailed t-tests are applied to compare the values indicated by asterisks to determine p-values.

FIGURE 8. PSA responses and exploratory biomarker correlations. Nadir PSA- the lowest PSA achieved on the clinical trial- for each patient were plotted in waterfall plot. Nadir (0.13) is indicated by the arrow. The A12 patient cohort was stratified into low PSA (better responders- blue lines) and high PSA (worse responders- red lines). The average and SEM values for the indicated biomarkers were measured as described in Figures 6 and 7 for the two groups. Fold-change is calculated as "low PSA" group average divided by "high PSA" group average. Statistical 2-sample, 2-tailed t-tests are applied to compare the values indicated by asterisks to determine p-values for these differences.

FIGURE 9. Body Mass Index effects on clinical outcome and biomarkers. Pre-treatment body mass index (BMI) for patients on the IMC-A12 study were calculated and displays in this waterfall plot. Using the PSA stratification shown in Figure 8, the pre-treatment BMI values for patients in the two PSA response groups were compared. Average is shown as a line with individual values in a scatter fashion. Statistical 2-sample, 2-tailed t-tests are applied to determine p-values for the two groups. Patients were stratified based on pre-treatment BMI and the serum biomarker results for patients in the low and high BMI groups were calculated to determine average and SEM values. Fold-change is calculated as "low BMI" group average divided by "high BMI" group average. Statistical 2-sample, 2-tailed t-tests are applied to compare the values indicated by the asterisks to determine p-values for these differences.

Figure 1. Effects of STC1 modulation on cell proliferation.

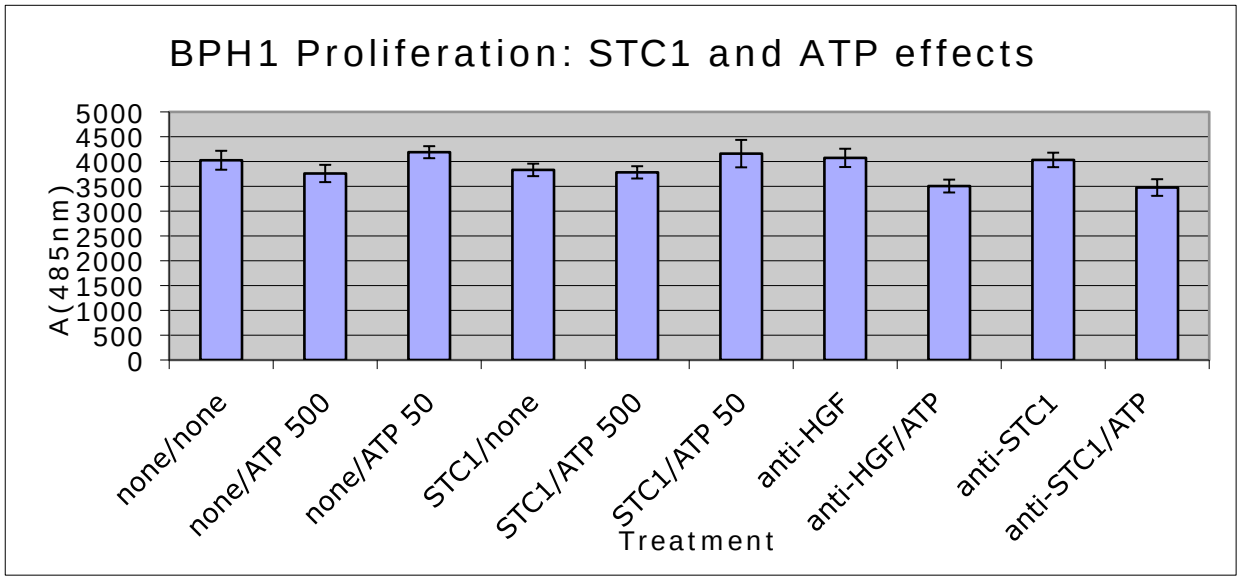

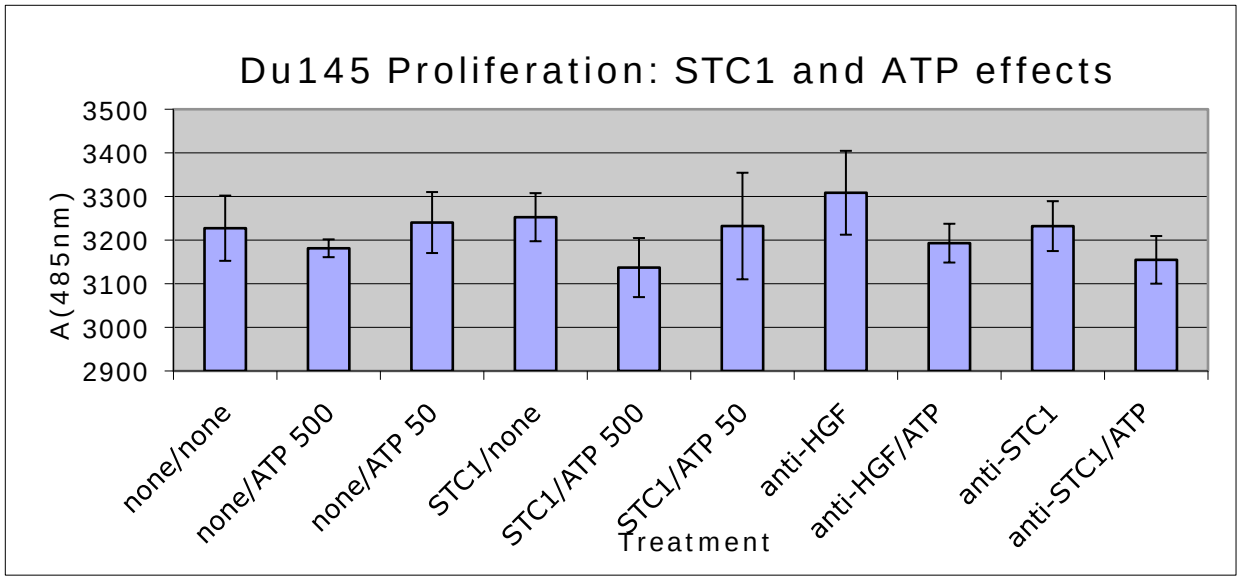

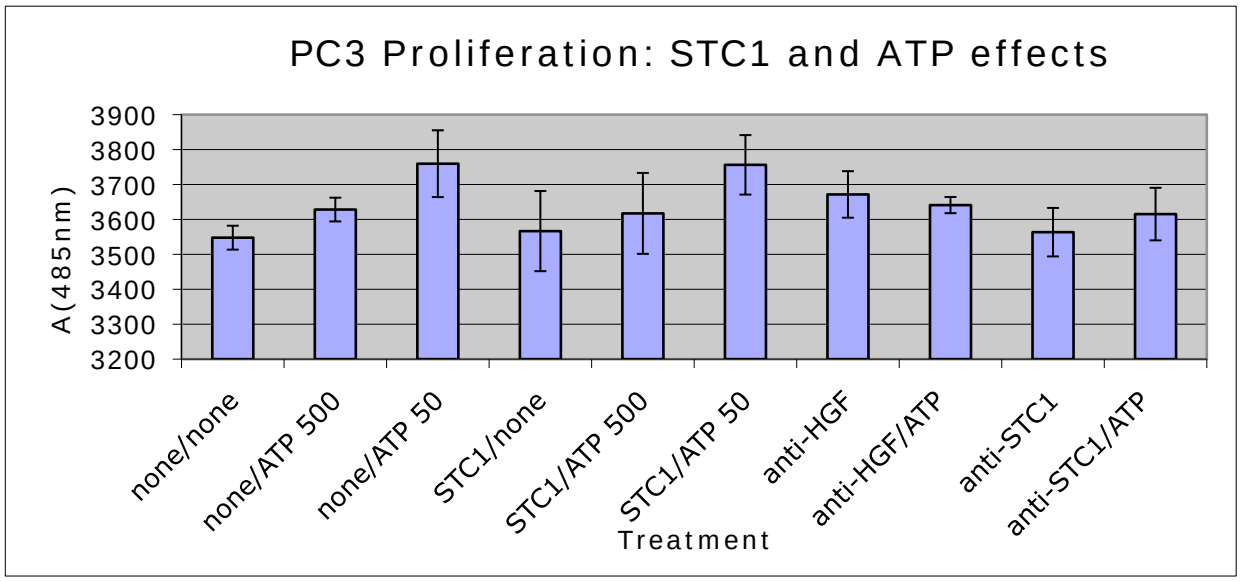

Figure 2. Effects of STC1 modulation on growth in Hypoxia.

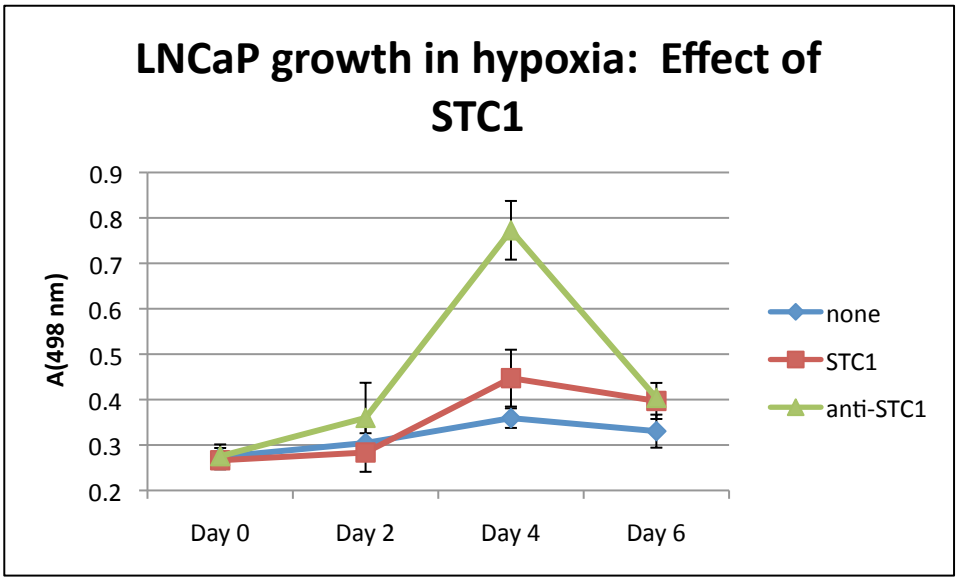

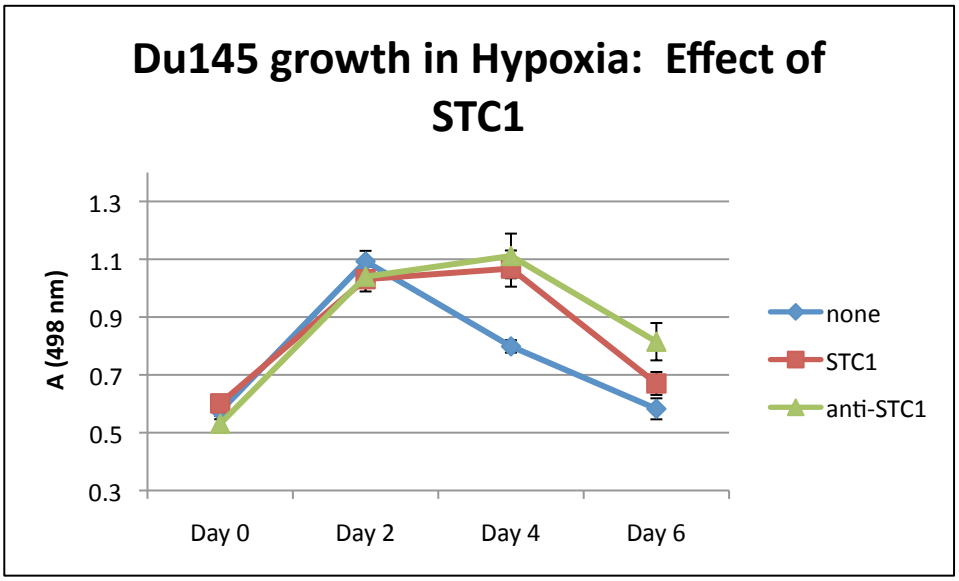

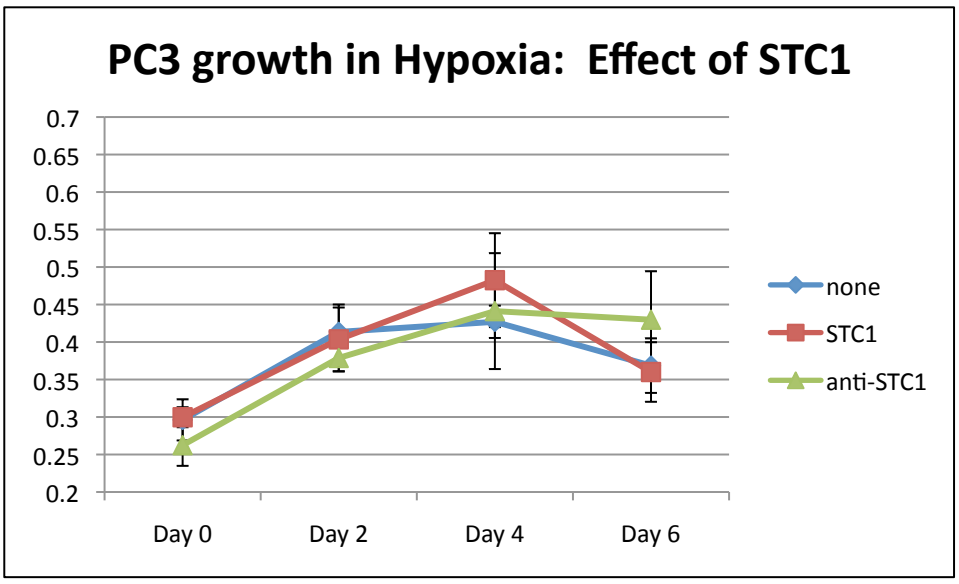

Figure 3. Effects of STC1 modulation on chemotherapy response.

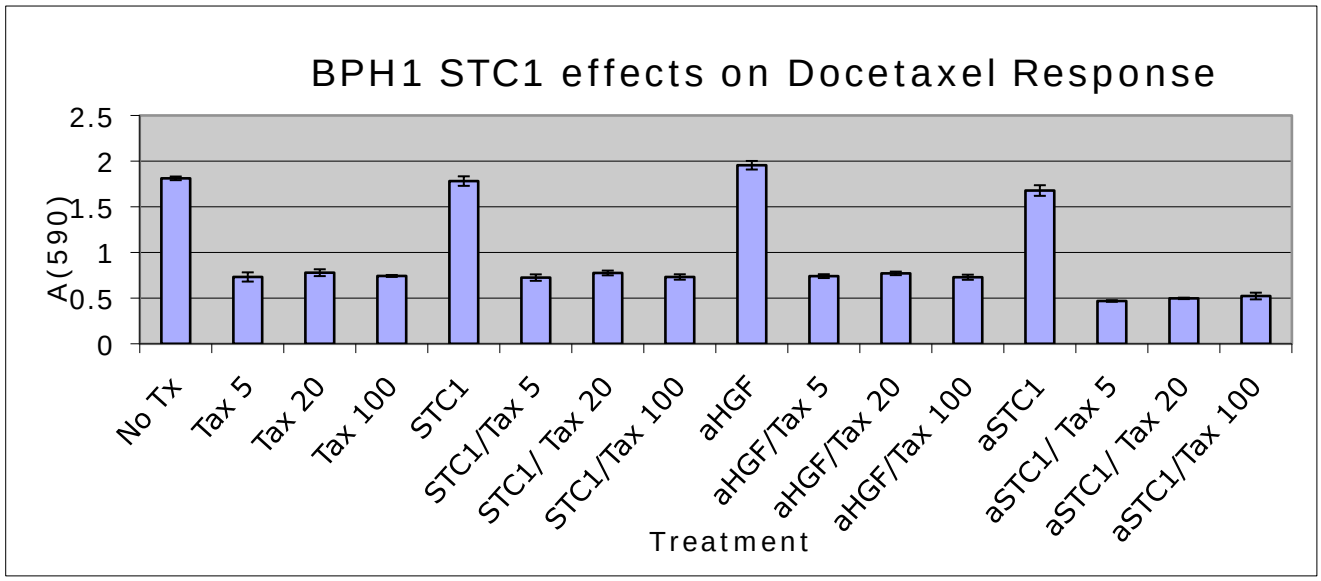

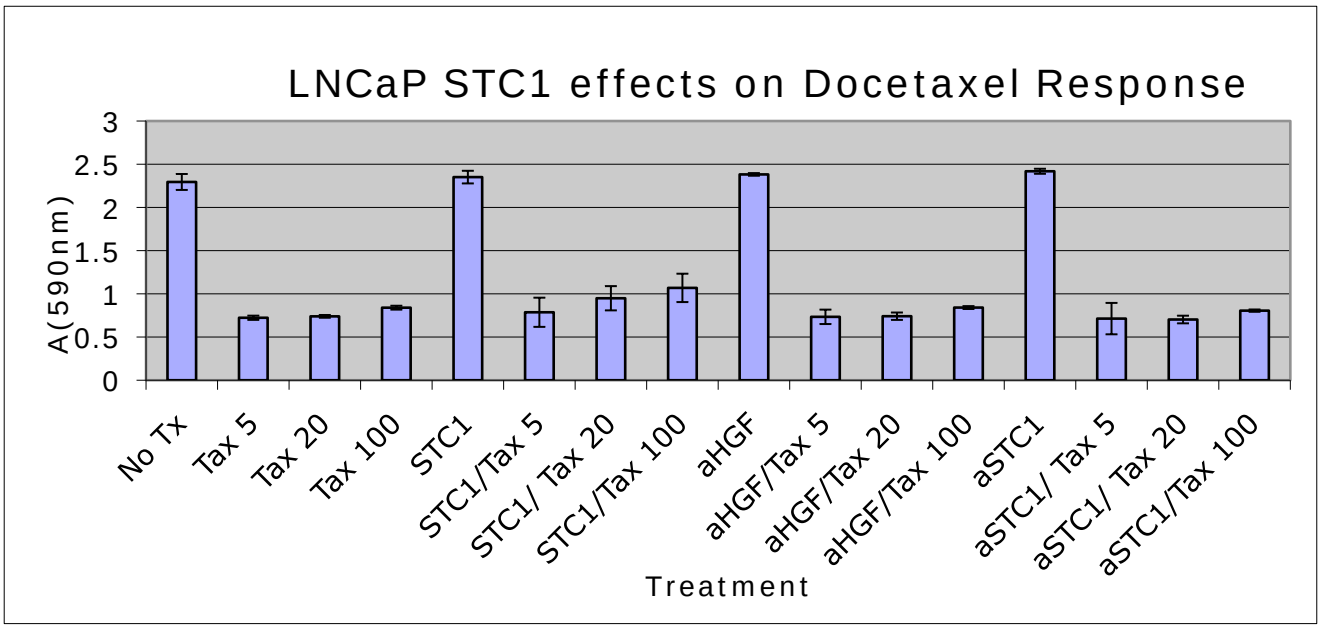

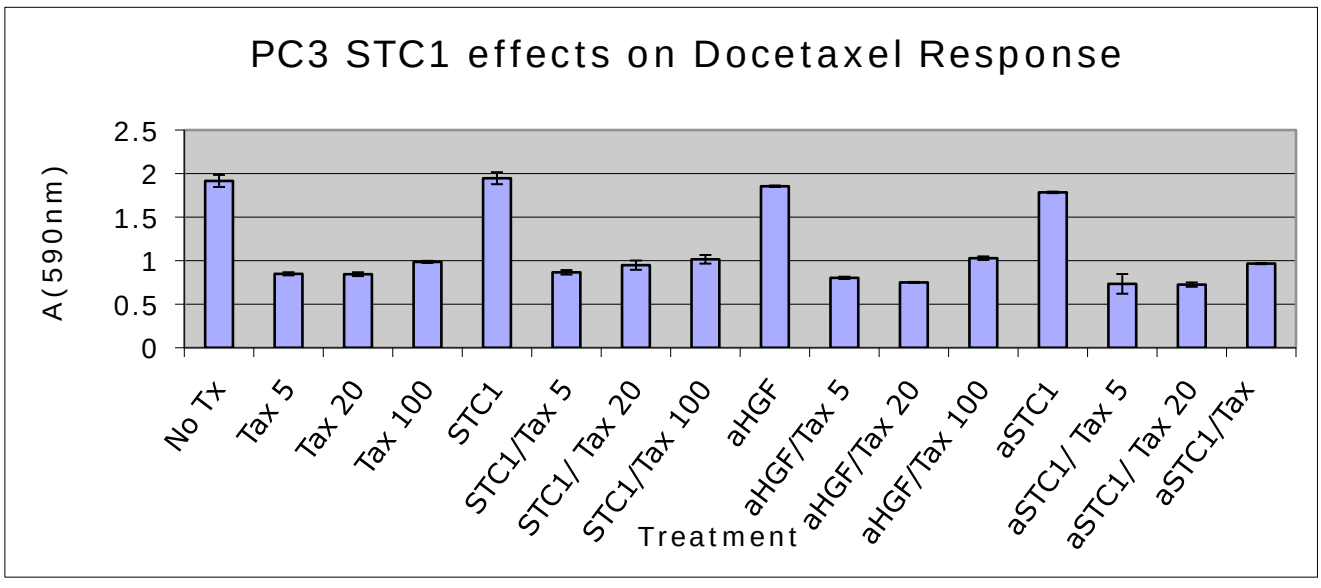

Figure 4. Effects of STC1 modulation on cell migration

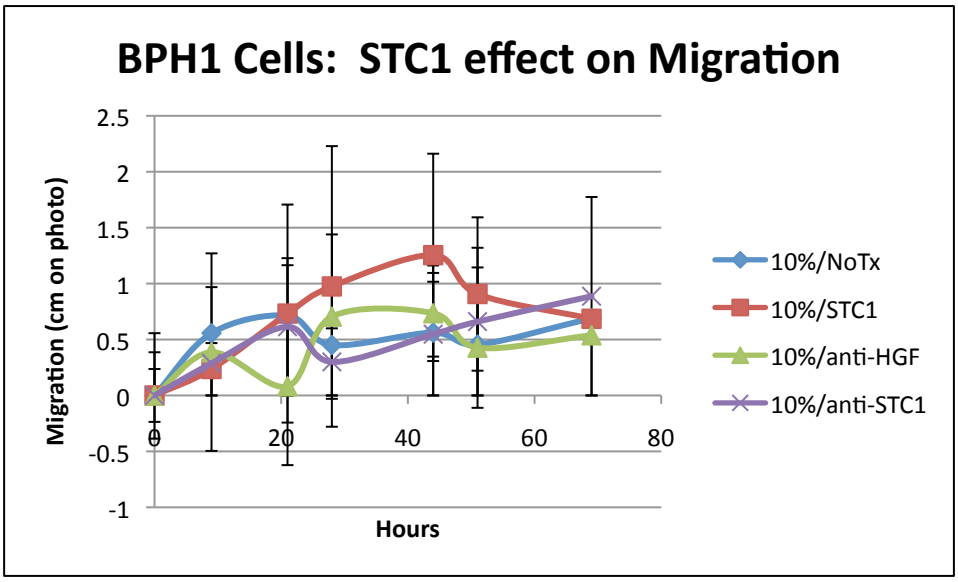

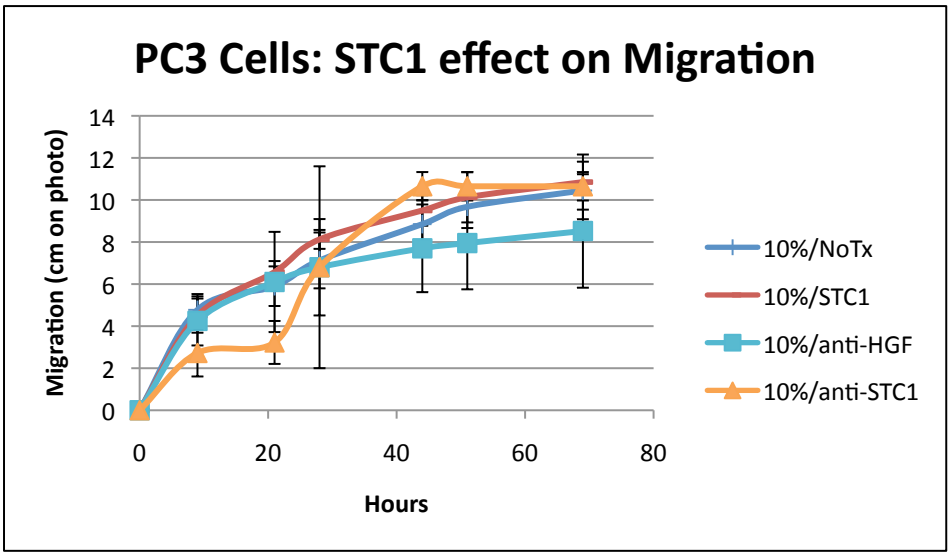

Figure 5. Expression of androgen metabolic genes by PC3 and LNCaP cell lines.

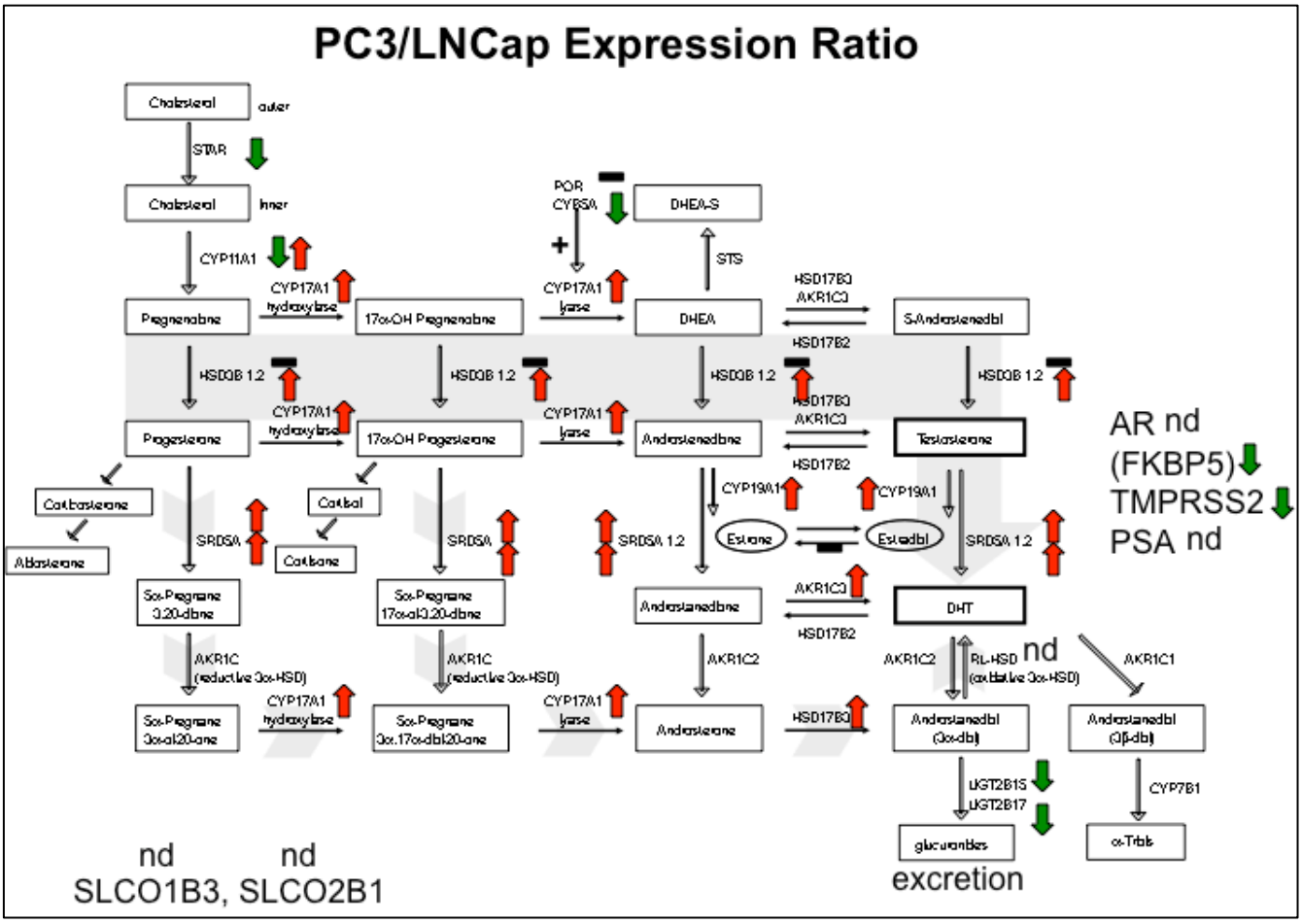

Table 1. Study patient Characteristics

Characteristic	A12		NeoADT	
	n	*Median*	*n*	*Median*
PSA		12		5.2
<10	8		11	
10-20	4		1	
>20	6		1	
Gleason Sum		4+4		4+3
3+4	3		5	
4+3	3		5	
4+4	7		1	
4+5	5		2	
Clinical T Stage		T2a		T2b
T1	4		2	
T2	8		8	
T3	6		3	
Body Mass Index		29.7		28
18.5-24.9	2		3	
25-29.9	9		7	
>=30	7		2	

Table 2. Clinical Pathological and Adverse Event Outcomes

SUMMARY OF PATHOLOGICAL OUTCOMES

- 1 Pathological Complete Response
- 17 pt. Tumor Stage- Similar to Kattan Predictions
- Lymph Node Positivity (6/18)- Similar to Kattan Predictions
- Positive Surgical Margins (4/18)

SUMMARY OF ADVERSE EVENTS

- Probably/Possibly related Grade 1/2 AEs:
  - Hyperglycemia/Diabetes requiring Metformin (2)
  - Asymptomatic Hyperglycemia/Diabetes
  - Skin Rash, Pruritis, Dry Skin
  - Diarrhea
  - Elevated AST
  - Hypertension
  - Increased Lacrimation
  - Blurry vision, Scotomata, Flashing lights
  - Tinnitis
  - Anemia, Thrombocytopenia, Neutropenia
- No Probably/Possibly related Grade 3/4 AEs
  - (Unrelated included peri-operative CVA, post-operative DVT/PE, HTN)

Figure 6. Effects of IGF-1R blockade and hormone therapy on IGF pathway homeostasis

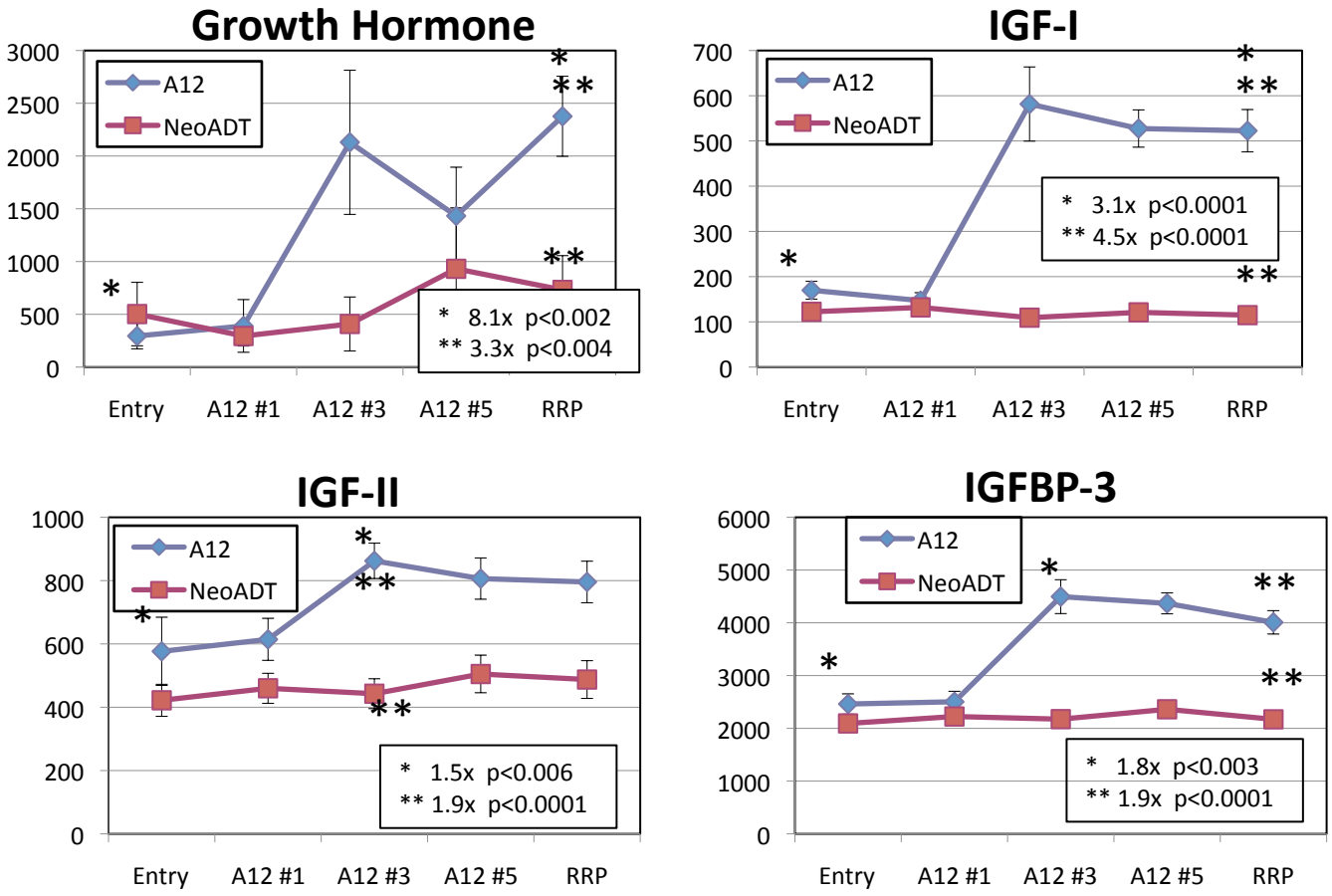

Figure 7. Effects of IGF-1R blockade and hormone therapy on glucose homeostasis and insulin activity

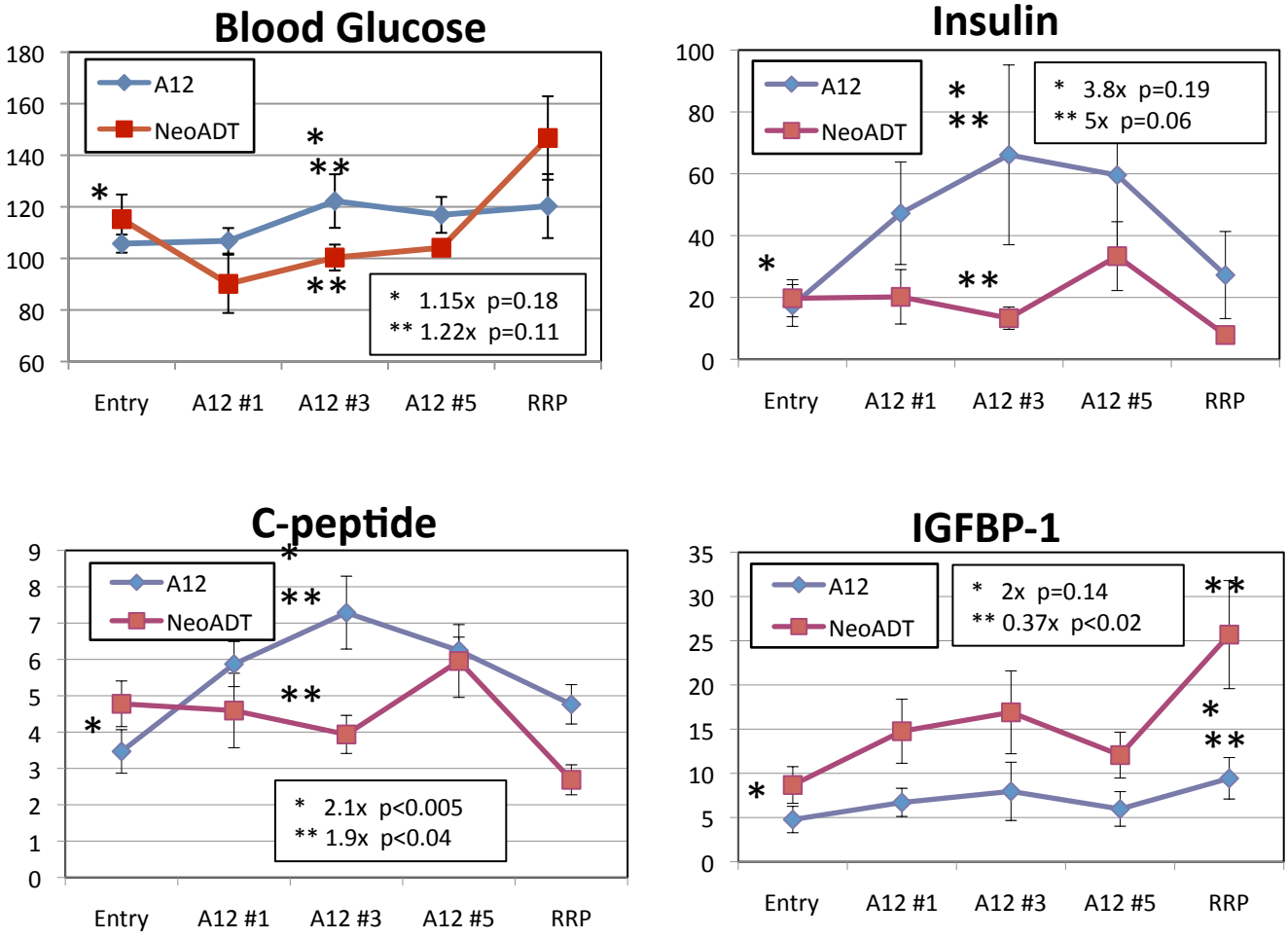

Figure 8. PSA responses and exploratory biomarker correlations

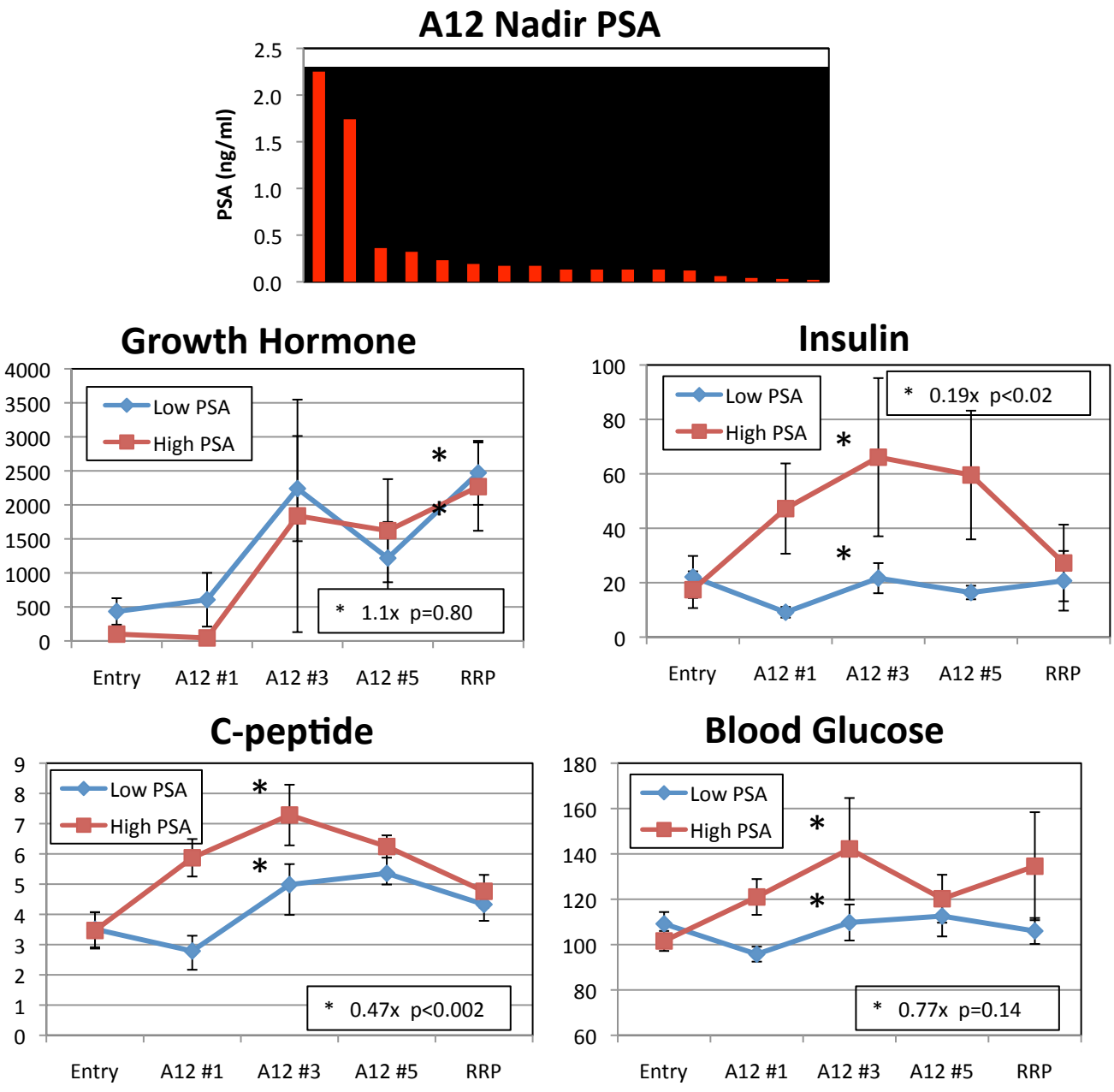

Figure 9. Body Mass Index effects on clinical outcome and biomarkers